Geoderma 289 (2017) 107–116

Contents lists available at ScienceDirect

Geoderma

journal homepage: www.elsevier.com/locate/geoderma

Spatial variation in the solute transport attributes of adjacent Typic Haplusteps, Mollic Ustifluvents, and Lithic Ustipsamments

Sabit Erşahin [a,*], Tayfun Aşkın [b], Ceyhan Tarakçıoğlu [b], Damla B Özenç [b], Kürşat Korkmaz [b], Turgut Kutlu [c], Seval Sünal [a], Bayram C Bilgili [d]

[a] Department of Forest Engineering, Faculty of Forestry, Çankırı Karatekin University, 18200 Çankırı, Turkey
[b] Department of Soil Science and Plant Nutrition, Faculty of Agriculture, Ordu University, 52250 Ordu, Turkey
[c] Department of Field Crops, Faculty of Agriculture and Natural Sciences, Bilecik Seyh Edibali University, 11210 Gülümbe, Bilecik, Turkey
[d] Department of Landscape Design and Architecture, Faculty of Forestry, Çankırı Karatekin University, 19200 Çankırı, Turkey

ARTICLE INFO

Article history:
Received 18 February 2016
Received in revised form 27 November 2016
Accepted 28 November 2016
Available online 8 December 2016

Keywords:
Pore-water velocity
Dispersivity
Miscible displacement
Semivariogram
Ordinary point kriging

ABSTRACT

Spatial variation in water flow and solute transport are important considerations when assessing field-scale remediation options, and for managing water and chemicals during agricultural production. Here, we evaluated the relationship between laboratory-measured solute transport variables pore-water velocity (v), dispersivity (λ), and retardation coefficient (R) and land use, soil type, and other independently measured soil properties in adjacent Typic Haplusteps, Mollic Ustifluvents, and Lithic Ustipsamments. We also characterized the spatial variation in v, R, coefficient of hydrodynamic dispersion (D), and λ. We obtained 100 geo-referenced, undisturbed soil columns (8.4 cm diameter and of varying length) from the topsoil at sites with varying land uses, topographies, and soil types, and synchronized disturbed soil samples to analyze the basic soil properties. We conducted miscible displacement tests on all 100 columns, and predicted the retardation coefficient (R) and D using the computer program CXTFIT, and measured v. All four variables, except R, had strongly right-skewed and kurtotic distributions, and were highly variable. Log λ (logarithm to base 10) was significantly correlated with land use, with the mean of λ being significantly greater in grasslands, followed by orchards and croplands. By contrast, v was significantly correlated with soil type, with the mean being significantly greater in Lithic Ustipsamments. Log v (logarithm to base 10) was also significantly correlated with the soil $CaCO_3$ content, log organic matter content, pH, cation exchange capacity, and log electrical conductivity, whereas neither v nor λ was correlated with soil texture measures. An analysis of the spatial structure of solute transport variables using semivariograms showed that R and λ had considerably high nugget effect. Log-transformed semivariograms performed well using ordinary point kriging for v and D. However, λ and R exhibited a very weak spatial dependency that could not be interpolated using ordinary kriging at the current sampling resolution. Therefore, this should be considered when designing future sampling programs to analyze spatial structure of R and λ.

1. Introduction

The capacity of soils to store and transport water and solutes is critical for hydrological and biochemical cycles (Kung et al., 2005). However, this capacity varies greatly at the landscape scale depending on land use, soil properties, and topographic characteristics (Nkedi-Kizza et al., 1983; Van Eijkeren and Loch, 1984; Anamosa et al., 1990). The solute transport parameters of agricultural topsoil are particularly important (Lessoff and Indelman, 2004), as they control the amount of nutrients that move beyond the root zone.

The general theory for the simultaneous transport of solutes and water considers physicochemical interactions between the solute and soil, which control water convection, hydrodynamic dispersion (D), anion exclusion, retardation, and solute degradation (Bresler and Laufer, 1974; Van Genuchten, 1981; Toride et al., 1995), all of which are highly variable in soils (Mulla and McBratney, 2002). Ward et al. (2004) suggested that these factors determine the solute arrival times in the groundwater, which should be considered when assessing field-scale remediation options. In addition, it is important to be able to predict these processes at an acceptable level of accuracy to evaluate the spatial distribution of contaminants and their migration to groundwater.

The distribution and magnitude of local variation in an attribute depends on the net effect of interactions between physical, chemical, and biological processes, with attributes that are affected by multiple factors exhibiting higher levels of spatial variability (Trangmar et al., 1985). Consequently, it is difficult to predict field-scale solute transport

* Corresponding author.
E-mail addresses: ersahin@karatekin.edu.tr, acapsu@gmail.com (S. Erşahin).

http://dx.doi.org/10.1016/j.geoderma.2016.11.035
0016-7061/

parameters (Costa and Prunty, 2006) because they are mediated by many different soil factors. For example, Biggar and Nielsen (1976) showed that it was difficult to predict the amount of solute moving beyond the root zone, and that pore-water velocity (v) and solute dispersivity (λ) exhibited a log-normal distribution with large variation; and further demonstrated that over 1000 samples were needed to predict a mean level of solute movement below the root zone that was within $\pm 10\%$ of the true mean. Kelleners et al. (1999) similarly stressed that K_s is an extremely variable soil property, and so this should be considered in field-scale solute transport modeling.

There are two main sources of uncertainty when determining a solute transport parameter in a landscape: 1) uncertainty due to measurement error and 2) uncertainty for locations where the subject attribute is not measured. The latter can be predicted using statistical techniques (Fetter, 1993). For example, for normally distributed data, the probability density function can be used to evaluate the heterogeneity of the attribute in the field, and the ergodic hypothesis may be applied to predict the value of the attribute with an uncertainty that depends on the standard deviation of its measured values (Fetter, 1993). However, when data show autocorrelation, geostatistical methods are often preferred for the spatial interpolation of solute transport attributes.

Geostatistics is a well-established branch of statistics that deals with spatial processes in a specific volume, known as the "support" (Isaaks and Srivastava, 1989; De Lucia et al., 2011). The semivariogram is one of the fundamental notions of geostatistics, being used to describe the spatial structure of an attribute between two distinct points of a domain as a function of the distance in between (Isaaks and Srivastava, 1989). The attribute may then be predicted in unobserved locations using the parameters (sill, range, and nugget) of the corresponding semivariogram (Isaaks and Srivastava, 1989).

Geostatistical techniques such as kriging can be used when the data are too scarce for modeling but sufficient for making spatial interpolation. The kriging technique has several advantages over its counterparts, including the fact that it incorporates the spatial structure of the data into the prediction through semivariogram modeling and predicts the same known values for the data points where measured data are available. In addition, geostatistical techniques can assist in the evaluation of the spatial structure of the subject variables and post-processing of the data (Corwin and Vaughan, 1997).

Numerous studies have related the results of solute transport studies to the parametric and morphological properties of soils at multiple scales (e.g., van Genuchten and Wierenga, 1977; Ersahin et al., 2002; Zhang and Gable, 2008); and the relationships between solute transport parameters have been studied by many authors (e.g., Bowman and Rice, 1986; Ward et al., 2004; Vanderborght and Vereecken, 2007). Starr et al. (1978) also investigated the effect of water application rate on the stability of solute flow in a layered soil. In recent decades, soil structural properties such as soil macropore features have received increased attention because preferential flow is the major driver behind the rapid movement of nonreactive and reactive chemicals, resulting in the contamination of groundwater and surface water systems. For example, Kung et al. (2005) characterized the size spectrum of macropores and preferential pathways in a field-scale leaching experiment, while Mossadeghi-Björklund et al. (2016) studied the effect of subsoil compaction on the preferential transport of bromide in a clay soil (Eutric Cambisol in the World Reference Base for Soil Resources (WRB) system).

Physical and biological factors that control the formation and destruction cycles of preferential pathways are highly variable both spatially and temporally (Kung et al., 2005). For example, when the soil is dry, a greater amount of water infiltrates into the soil matrix and less macropore flow occurs (Vanclooster et al., 2005). Flury et al. (1994) studied the effect of initial water content on the generation of preferential flow in well-structural soils. A comprehensive literature review was conducted by Vanderborght and Vereecken (2007). They discussed dispersivities, obtained in column-, liysimeter-, and field-scale studies, in regard with flow rate, soil texture, travel distance, and boundary conditions of the experiments. Another comprehensive study was conducted by Koestel et al. (2012), who acquired 733 breakthrough curves (BTCs) under steady-state saturated conditions from peer-reviewed literature and related the BTC-shape measures to experimental boundary conditions, soil properties, and site factors.

A literature search revealed that there have been an inadequate number of geostatistical analyses of the spatial variation of solute transport parameters, which we attributed to the high cost- and time-consuming nature of solute transport studies. Therefore, in this study, we aimed 1) to evaluate pore-water velocity (v),retardation coefficient (R), and dispersivity (λ) as affected by soil properties in an area of adjacent Typic Haplusteps, Mollic Ustifluvents, and Lithic Ustipsamments that used as grassland, cropland, and orchard and 2) to model the spatial structures of v, coefficient of hydrodynamic dispersion (D), R, and λ using semivariograms and to interpolate these in the topsoil (A horizon) of the study area. We found that v and D had a clear spatial structure that allowed their successful interpolation using the ordinary kriging (OK) technique with the applied sampling scheme, while both R and λ had a very weak spatial dependency that did not allow their spatial interpolation by OK.

2. Theory and calculations

A one-dimensional convection-dispersion equation (CDE) is widely used in solute transport studies (Van Genuchten, 1981; Parker and van Genuchten, 1984; Toride et al., 1995). For a reactive solute (e.g., potassium), the one-dimensional CDE has the form:

$$R\frac{\partial c}{\partial t} = D\frac{\partial^2 c}{\partial x^2} - v\frac{\partial c}{\partial x} \tag{1}$$

where R is the retardation coefficient ($=1-(D_bK_d/\theta)$, where D_b is the soil bulk density, K_d is the solute distribution coefficient between the solid and liquid phases, and θ is the volumetric water content of the porous medium), c is the solute concentration (ML^{-3}), D is the coefficient of hydrodynamic dispersion (L^2T^{-1}), t is time (T), v is the average linear pore-water velocity (LT^{-1}), and x is distance (L) (Van Genuchten, 1981; Toride et al., 1995). This equation assumes that water flow in the system is in a steady-state and that water content is constant throughout the porous system (Van Genuchten, 1981; Parker and van Genuchten, 1984). In theory, R is assumed to be 1.0 for a nonreactive solute.

The following dimensionless variables have been introduced to analyze effluent data (Parker and van Genuchten, 1984):

$$T = vt/L \tag{2}$$

$$z = x/L \tag{3}$$

$$P = vL/D \tag{4}$$

$$C/C_0 = (c - C_i)/c_0 - C_i) \tag{5}$$

where, P is a dimensionless Peclet number, C_i is the initial concentration of the tracer in the soil, c is the concentration of the tracer measured at distance x, c_0 is the tracer concentration in the stock solution, t is the time elapsed from the start of the tracer application, C/C_0 is the dimensionless concentration of the tracer at $x = L$, T is the dimensionless number of pore volumes with the tracer, and z is the dimensionless depth.

Eq. (1) implies that the coefficient of hydrodynamic dispersion (D) and pore-water velocity (v) are the principal variables controlling the transport of a conservative tracer (e.g., bromide) in soils and similar porous media (e.g., sand and glass beads columns). However, dispersivity [$\lambda(L) = D/v$] is also frequently used to determine whether the transport is convective or dispersive dominated (Parker and van Genuchten, 1984; Toride et al., 1995).

3. Materials and methods

3.1. Study area

The study area was located in the middle Black Sea region of Turkey (Fig. 1), which is characterized by mild, rainy winters and warm, humid summers (Iyigun et al., 2013). The area is 5539 ha in size and bordered by the Black Sea in the north, and by footslopes and backslopes of varying heights in the south, and is designated as toeslope and footslope according to the hillslope model (Schoeneberger et al., 2002). The slope gradually decreases toward the Black Sea coast to the north, becoming completely flat near to the shore. The soil characteristics in this area vary depending on the steepness and position of the slopes, and the applied management practices. Soils on the toeslopes are Mollic Ustifluvents, while those on the footslopes are finer textured Typic Haplusteps (Fig. 1a). Soils closer to the seaside have a lithic contact to sand at approximately 20 cm below the surface, with the depth of sand becoming shallower and the soils becoming coarser toward the shore, and so are designated as Lithic Ustipsamments. The studied soils have been used as grassland, and to grow field crops such as corn, soybean, and alfalfa, and fruits such as cherry, peach, hazelnut, and apple orchards (Fig. 1b). Conventional tillage is applied in the cultivated areas. Table 1 shows some of the morphological properties of the soils that were commonly observed during sampling.

3.2. Soil sampling and laboratory analyses

We randomly sampled 100 undisturbed soil samples using a tractor-powered hydraulic column sampler in late October 2011. We selected the sampling sites based on their topography, soil management, soil type, and proximity to the shore. (Note: we did not sample any localities within 100 m of the shore because the sand layer was too close to the soil surface, and even exposed in some places.) Each sampling site was georeferenced using a Global Positioning System (GPS) with a precision of ±1 m. Undisturbed soil samples were taken using 8.4-cm diameter plastic tubes located in a steel sampler. The sample depths varied depending on the vertical soil conditions, with the depth being limited by subsurface stones at some sites and sand located below 20 cm at other sites closer to the shore. A field observation chart was filled out at each sampling site, which included information such as soil use, and soil morphological features (e.g., macropores, roots, soil structure, concretions, surface coatings, and redoximorphic features, if any). Field observations were made following the procedure and guidance provided by Schoeneberger et al. (2002). Some of the common features that were observed in most of the soil samples are given in Table 1.

Both ends of the soil columns were sealed at the time of sampling to prevent any moisture loss, which would cause defects in the soil structure. In addition, synchronized disturbed soil samples were taken to measure the organic matter content, cation exchange capacity (CEC), particle-size distribution, soil $CaCO_3$ content, pH, and electrical conductivity (EC). The soil samples were transported to the laboratory and stored at room temperature for analysis.

All 100 disturbed soil samples were analyzed for clay, silt, and sand content using the hydrometer method (Gee and Bouder, 1986), for organic matter content using the Walkley-Black method (Nelson and Sommers, 1982), for soil pH and $CaCO_3$ using the methods in McLean (1982), for CEC using the method given by Rhoades (1982a), and for EC using a glass electrode (Rhoades, 1982b). The water contents at soil water pressures of −0.033 MPa ($\theta_{-0.033\ \mathrm{MPa}}$) and −1.50 MPa ($\theta_{-1.50\ \mathrm{MPa}}$) were measured using a pressure plate apparatus (Cassel and Nielsen, 1986), and the saturated hydraulic conductivity of the undisturbed soil columns was measured using a Marriotte's bottle under a zero soil water pressure head (Klute and Dirksen, 1986). All of the soil analyses except bulk density (D_b) and K_s (measured on undisturbed soil columns) were conducted in duplicate.

3.3. Miscible displacement tests

Before conducting a miscible displacement test, the lower end of the soil column was supported with a fabric. The column was then gradually

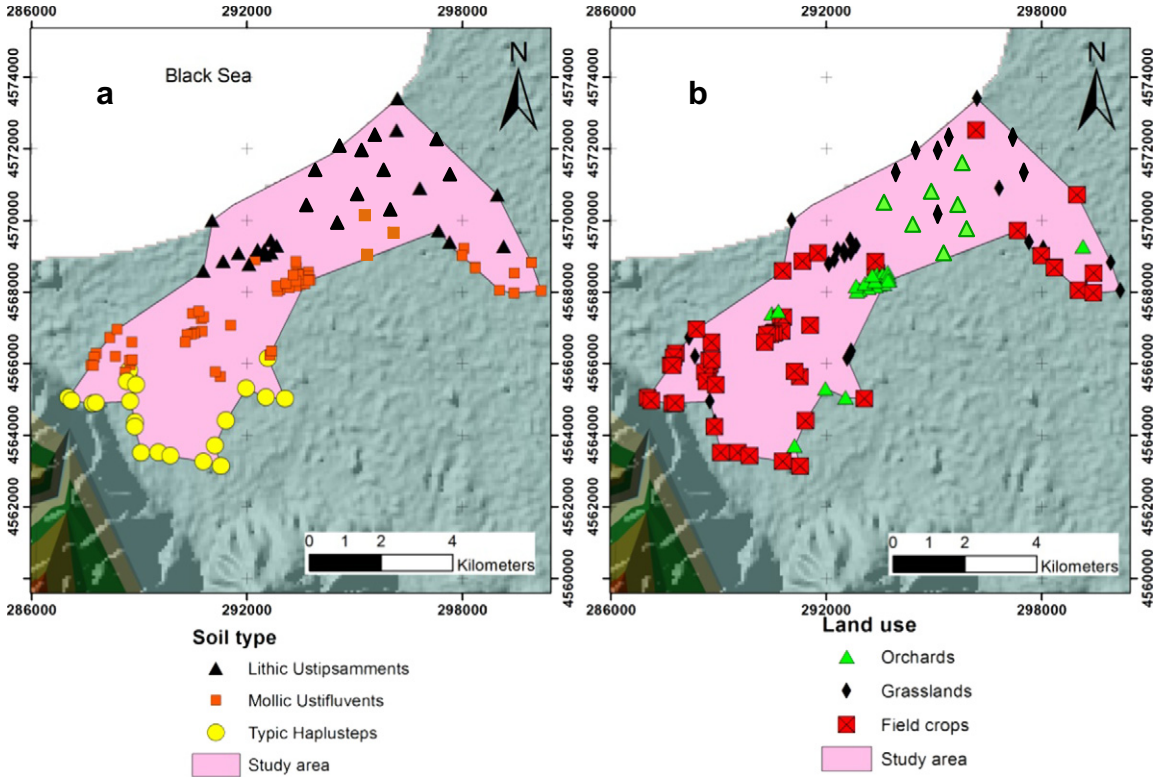

Fig. 1. Location of study area showing distribution of sampling points by soil type (a) and by land use (b).

Table 1
Some morphologic features commonly observed on soils at different land uses and soil types in the study area.

Land use	Morphologic features	Soil type[a]
Corn, irrigated	Moderate, medium, granular structure; many fine roots; irregular, common, medium, vesicular pores in the upper 15 cm. Strong, coarse, columnar structure; few, continuous, earthworm channels; few, coarse roots from upper horizon in 15–30 cm.	MU
Grassland, grazed	Strong, medium, granular structure; many, fine, roots; many, fine, vesicular pores in the top 13 cm. Strong, coarse, angular blocky structure; very few, coarse, dentritic tubular pores; vertically oriented few coarse roots in the 13–30 cm.	MU
Grassland, grazed, approximately 100 m to the sea	Weak, fine, granular structure; many fine roots; many, fine vesicular pores in the top 8 cm. Structureless sand, few fine-to coarse roots, some vesicular pores with low vertical continuity in the 8–30 cm depth.	LU
Apple orchard, tilled, drop irrigated	Moderate, medium, subangular blocky structure; common, fine roots, throughout; common, medium, dentritic tubular pores in 0–20 cm. Moderate, medium, angular, blocky structure; many, fine to coarse roots, between peds; few, medium, dendritic tubular pores in 20–35 cm.	TH
Apple orchard, not tilled for three years.	Strong, medium, subangular blocky structure; common, medium roots, throughout; common, dendritic, pores and very few tubular (earthworm channels) in the upper 0–10 cm. Strong, medium, subangular blocky structure; common, medium roots, throughout; common, coarse, dentritic root channels and few tubular earthworm channels with high vertical continuity in the 10–30 cm.	MU
Hazelnut orchard, not tilled for three years.	Moderate, medium, subangular blocky structure; many, very fine, roots throughout; many, vesicular pores in the 0–10 cm. Moderate, coarse, subangular blocky structure; common, medium, pores between peds; common, medium, irregular pores with low vertical continuity in 10–30 cm.	TH
Alfalfa, sprinkler irrigated	Weak, medium, fine, granular structure; common, fine, roots throughout; common, medium, vesicular pores in 0–15 cm. Moderate, medium, angular, blocky structure; many, fine-to moderate roots in cracks; very few, dendtritic pores with low continuity in 15–30 cm.	MU

[a] MU: Mollic Ustifluvents, TH: Typic Haplusteps, LU: Lithic Ustipsamments.

saturated with a 0.01 N $CaCl_2$ solution from the bottom (van Genuchten and Wierenga, 1977) in a container. To avoid evaporation from the column, a plastic cover was placed over the top of the container. Upon saturation, the column was positioned on an upright stand and the inlet at the top of the column was connected to a Marriotte's bottle. Once a steady-state flow had been established under a zero soil water pressure head, approximately five pore volumes of tracer solution (0.05 N KBr in 0.01 M $CaCl_2$ solution) were introduced to the column at a zero soil water pressure head using another Marriotte's bottle. The effluent was collected with a fraction collector and analyzed for bromide with a bromide-specific electrode (Abdalla and Lear, 1975).

Following the miscible displacement test, the column was taken and left to dry for 3 days in the laboratory, following which small undisturbed samples were taken from the upper and lower ends of the column using steel rings (1.0 cm depth and 10.8 cm^2 surface area). These undisturbed samples were then used to measure the field capacity of the column in a pressure plate apparatus, whereas disturbed soil samples were used to measure the wilting point of the soils in the pressure plate apparatus. The column containing the rest of the undisturbed soil was then placed in an oven at a constant temperature of 105 °C to measure its dry bulk density, which was used to calculate the total porosity (f):

$$f = 1-(D_b/D_p) \quad (6)$$

where, D_b is the bulk density (ML^{-3}) of the column and D_p is the density of particles (ML^{-3}). As the organic matter content of the soils was not high enough (<5%) to affect mean particle density, the D_p was simply assumed to be 2.65 Mg m^{-3}, which is the typical value for mineral soils. The saturated water content (on a volume basis, θ_s) of the column during the test was assumed to be equal to its total porosity.

Dimensionless concentrations (C/C_0) of bromide were calculated by dividing the concentration of bromide in the effluent (C) by the concentration in the stock solution (C_0), both of which were measured using the same bromide-specific electrode. The bromide in the stock solution was measured rather than calculated to minimize the error arising from differences between the calculation (stock solution) and measurement (collected effluents). Similarly, dimensionless pore volumes (P/P_0) were calculated by dividing the cumulative volume of effluent collected (P) by the pore volume of the column (volume of effluent in the saturated column, P_0). A breakthrough curve (BTC) was then plotted for each column with C/C_0-values on the y-axis and the corresponding P/P_0-values on the x-axis.

Data from the miscible displacement tests were modeled using a CDE model and the BTCs were modeled using the computer program STANMOD (Šimůnek et al., 1999). The parameter v was measured in the columns, while D and R were predicted using the CDE model. In theory, the parameter R is assumed to be 1.0 for a non-reactive solute. However, we also predicted R, as some breakthroughs indicated that some of the R-values were highly deviated from unity (value of P/P_0 at $C/C_o = 0.5$).

3.4. Statistical and geostatistical analyses

Exploratory data analysis was conducted, and the distributions of the solute transport attribute data were described by calculating the mean, standard deviation, coefficient of variation, skewness, and kurtosis. Webster (2001) suggested that data with a skewness >|1.0| are highly skewed and so a log-transformation may be used to make them normally distributed, data with a skewness between |0.5| and |1.0| are moderately skewed and so may be square-root transformed, and data with a skewness <|0.5| are slightly skewed and so can be considered normally distributed. Based on this suggestion, we log-transformed (logarithms to base 10) the strongly skewed data for v, D, and λ, and then recalculated the descriptive statistics based on these transformed data (Cambardella et al., 1994).

We used the geostatistical software GS+ (Gamma Design, St. Plainwell, MI) to analyze the spatial structure of the data for each parameter, to model semivariograms, and to conduct ordinary kriging interpolations. We computed semivariances for v, D, and λ using log-transformed data to minimize the effect of extreme values, and selected the semivariogram models with the highest R^2-values and lowest SSE-values (Cambardella et al., 1994). However, the semivariogram for R was computed using untransformed data since data were normally distributed (Table 2). Variable lag distances were also used to select semivariograms, whereby at least ten lags were used, with a minimum of 30 data pairs ensured in each lag. We conducted ordinary point kriging (OK) interpolations using the parameters from the corresponding semivariograms that were computed using log-transformed data for v, D, and λ, and untransformed data for R. A minimum of 10 and a maximum of 13 neighbors within the geostatistical range were allocated in the kriging predictions. A cross-validation test was applied before kriging (Isaaks and Srivastava, 1989), and the cross-validation correlation coefficient and relative mean absolute error (RMAE) (Armstrong and Collopy, 1992) calculated using residuals of cross-validation were

Table 2
Descriptive statistics for retardation coefficient (R) and log-transformed (logarithms to base 10) values of pore-water velocity (v), coefficient of hydrodynamic dispersion (D), and dispersivity (λ).

Variable	Mean	SD	CV	Skewness	Kurtosis
v (cm h^{-1})	6.51	10.33	1.59	2.91	9.16
Log v	1.08	1.22	1.13	0.32	−0.13
D (cm^2 h^{-1})	8.84	18.36	2.08	5.14	32.46
Log D	1.24	1.53	1.23	−0.07	0.89
λ (cm)	1.64	1.46	0.88	2.92	10.51
Log λ	0.20	0.81	2.00	−0.68	2.05
R	1.01	0.12	12.0	0.48	−0.02
R^2	0.98	0.01	1.34	−1.14	0.73

SD: standard deviation, CV: coefficient of variation, R^2: coefficient of determination for parameter estimation by CDE.

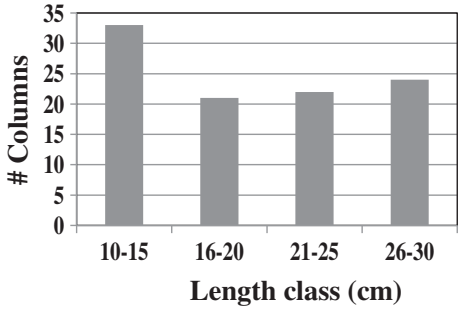

Fig. 2. Length (cm) distribution of the 100 undisturbed soil columns used in the miscible displacement tests.

used as criteria in the evaluation of interpolation accuracy. The log-values of variables were back transformed to produce the final maps (Gregory et al., 2006).

4. Results

4.1. Soil properties

Soil pH showed a strongly left-skewed and slightly kurtotic distribution (Table 3) according to the criteria of Webster (2001). By contrast, the sand, silt, and clay contents of the soil varied moderately and had a slightly right-skewed distribution (Table 3). These results support those that were previously reported by Mulla and McBratney (2002). Soil aggregate stability (AS) also varied moderately, ranging from 0.12 to 0.98 (dimensionless) (Table 3), whereas the D_b of the studied soils was highly variable. Low to medium CV-values have previously been reported for D_b (e.g., Mulla and McBratney, 2002). This high level of variation in D_b in our study was attributed to differences in soil type and land use (Fig. 1, Table 1).

4.2. Solute transport variables

Miscible displacement tests were conducted on all 100 undisturbed soil columns. The internal diameter of the columns was 8.5 cm, but their lengths varied depending on the topsoil thickness and other soil conditions, such as the presence of stones. The mean column length was 18.8 cm (± 6.09 cm SD), and the column length had a slightly right-skewed and negatively kurtotic distribution. The Fig. 2 shows that more than half of the columns had a length < 20 cm. The property R had a slightly right-skewed distribution, while v and λ had a strongly right-skewed and highly positively kurtotic distribution (Table 2). Our CV-values for the solute transport variables v and λ were within the ranges previously reported by Mulla and Mc Bratney (2002).

The parameter log v was significantly correlated with CEC, pH, log EC and log $CaCO_3$ content (Table 4). Neither log v nor log λ was significantly correlated with the physical properties of the study soils. On the other hand, log λ was also significantly but weakly correlated with land use (Table 4), and analysis of variance (ANOVA) revealed that log λ was significantly greater in grasslands followed by orchards and croplands.

Values for R ranged from 0.68 to 1.30 with a mean of 1.01 and standard deviation of 0.12. The values <1.0 could have resulted from anion exclusion, preferential flow, or both, while those > likely resulted from adsorption due to pH-dependent positive charges on the particles at a low pH (Sposito, 2008). Gupte et al. (1996) similarly reported anion adsorption in their 40 Cecil Sandy Loam columns (clayey, kaolinitic, thermic Typic Kanhapludult).

We evaluated the spatial structure of R, log D, log v and log λ using semivariograms (Fig. 3 and Table 5). All semivariograms were bounded (i.e., had a sill). A bounded semivariogram indicates that second order stationarity exists, while an unbounded semivariogram indicates a general trend in the spatial structure and/or a lack of second-order stationarity (Isaaks and Srivastava, 1989; Matias et al., 2005). According to Cambardella et al. (1994), an attribute with a nugget/sill of <0.25 is deemed strongly spatially dependent, of 0.50–0.75 is moderately spatially dependent, and of >0.75 is weakly spatially dependent. Thus, our semivarograms for log v was moderately and log D was strongly spatially dependent, while those for R and log λ were weakly spatially dependent (Table 5).

All semivariograms had nugget values >0, suggesting that there were small-scale variations in the solute transport attributes. These will have been related to several factors, including differences in micro-topography, other small-scale patterns that could not be detected by the sampling scheme used, errors in the accuracy of the sample locations recorded using the GPS, and errors in the laboratory measurements (Gregory et al., 2006).

The geostatistical range is the distance within which the solute transport attributes are autocorrelated. The attribute log v had long geostatistical range, indicating that the processes controlling its distributions resulted in a more differential spatial scaling and that regional spatial patterns were predominant (Gregory et al., 2006). The correlation coefficients between the predicted and measured values during cross-validation ranged from 0.02 for log λ to 0.87 for log D (Table 5).

We interpolated D- and v-values using ordinary point kriging (OK), and mapped these kriging-interpolated values (Fig. 4). Both variables had reasonably low relative mean absolute error (RMAE) and high cross-validation correlation coefficient (Table 6), indicating that OK successfully interpolated them. The interpolated (Table 6) and measured (Table 2) values for D and v were highly similar in terms of their means and standard deviations. By contrast, λ and R had almost pure nugget variance (Fig. 3). Therefore, we mapped these using the normal distance weighted method, as they were very weakly spatially dependent (Fig. 4).

Table 3
Descriptive statistics of some soil properties in the study area ($n = 100$).

	Mean	SD	Min.	Max.	CV (%)	Skewness	Kurtosis
Sand (%)	41.20	14.21	15.00	76.00	34.49	0.18	−0.56
Silt (%)	17.93	5.25	9.00	33.72	29.30	0.43	0.22
Clay (%)	40.35	14.49	4.28	74.00	35.90	0.057	−0.54
CEC ($cmol_c$ kg^{-1})	35.29	10.40	3.98	57.47	29.48	−0.50	0.83
pH	7.59	0.60	5.73	8.55	7.91	−1.21	0.80
EC (mmhos cm^{-1})	143.1	98.82	38.3	484.0	69.03	1.53	1.69
OM (%)	2.71	0.96	0.04	4.91	35.17	−0.01	0.56
$CaCO_3$ (%)	3.32	2.95	0.10	12.65	88.91	1.08	0.40
D_b (Mg m^{-3})	1.30	0.13	1.03	1.58	9.69	0.16	−0.58
AS (−)	0.64	0.16	0.12	0.98	24.04	−0.48	0.33
FC (%)	39.48	6.45	19.75	50.74	16.34	−0.90	1.08
WP (%)	26.10	6.90	0.21	43.85	26.44	−0.65	1.51
f (−)	0.51	0.054	0.39	0.64	10.82	−0.11	−0.50

SD: standard deviation, CV: coefficient of variation, CEC: cation exchange capacity, EC: electrical conductivity, OM: organic matter, D_b: bulk density, AS: aggregate stability, FC: field capacity (volumetric), WP: wilting point (volumetric), f: total porosity, −: unitless.

Table 4
Correlations among the studied attributes ($n = 100$).

	Sand (%)	Silt (%)	Clay (%)	CEC	pH	Log EC	OM	Log $CaCO_3$ (%)	FC	WP	D_b	*R*	Log *v*	Log *D*	Log λ	LU
Silt	−0.186															
Clay	−0.88**	−0.22*														
CEC	0.22*	−0.14	0.20*													
pH	0.05	−0.15	0.01	−0.18												
Log EC	0.09	−0.08	−0.09	0.60**	−0.16											
OM	−0.05	0.05	0.04	0.52**	−0.27*	0.30**										
Log $CaCO_3$	−0.02	0.01	0.03	−0.42**	0.47**	−0.24*	−0.50**									
FC	−0.06	0.06	0.08	0.02	0.13	−0.04	0.22*	0.07								
WP	−0.11	0.04	0.11	0.12	0.01	0.08	0.23*	−0.02	0.65**							
D_b	−0.10	−0.03	0.15	−0.17	0.14	−0.24*	−0.01	0.17	0.03	0.11						
R	−0.02	0.02	0.02	0.17	−0.25**	0.13	0.28**	−0.23*	0.05	0.08	−0.14					
Log *v*	0.04	−0.03	−0.04	−0.24*	0.30**	−0.41**	−0.18	0.28*	0.02	0.03	0.10	−0.11				
Log *D*	−0.04	0.04	0.01	−0.20*	0.21*	−0.39**	−0.15	0.21*	0.04	0.07	0.12	−0.10	0.82**			
Log λ	−0.13	0.12	0.07	0.02	−0.08	−0.06	0.01	−0.05	0.04	0.09	0.07	−0.01	−0.06	0.51**		
LU	0.04	−0.10	0.03	−0.16	−0.32**	−0.29**	0.07	0.12	0.17	0.13	0.04	0.04	0.15	0.29**	0.29**	
ST	0.22*	−0.06	−0.19	−0.39**	0.42**	−0.41**	−0.25*	0.17	0.06	−0.04	0.14	−0.24*	0.15	0.33**	−0.06	0.31**

CEC: cation exchange capacity ($cmol_c\ Kg^{-1}$), EC: electrical conductivity ($mmhos\ cm^{-1}$), OM: organic matter (%), FC: field capacity ($m^3\ m^{-3}$), WP: wilting point ($m^3\ m^{-3}$), D_b: bulk density ($Mg\ m^{-3}$), *v*: pore-water velocity ($cm\ h^{-1}$), *D*: coefficient of hydrodynamic dispersion ($cm^2\ h^{-1}$), λ: dispersivity (cm), R: retardation coefficient (dimensionless), LU: land use, ST: soil type. The logarithms are to base 10. The soil type was coded as follows: Typic Haplusteps = 1, Mollic Ustifluvents = 2, and Lithic Ustipsamments = 3; and land use was coded as follows: field crops = 1, orchards = 2, and grasslands = 3.

* Significant at 0.05.

** Significant at 0.01 level of significance.

5. Discussion

5.1. Correlations among the studied attributes

None of the solute transport variables (*R*, log *v*, or log λ) were correlated with soil physical properties, sand, silt, and clay contents, D_b, field capacity, or wilting point (Table 4). Furthermore, there were no significant correlations with any of the soil textural components, despite these being moderately variable (Table 3). By contrast, Koestel et al. (2012) found a significant negative correlation between *v* and the soil silt and OM contents, and a significant positive correlation between *v* and the sand content of 733 columns from peer-reviewed literature; and also reported that dispersivity (λ) was significantly negatively correlated with sand content and positively correlated with silt and clay contents in their columns. Similarly, Ghafoor et al. (2013) reported significant correlations between preferential transport and clay content, and Kazemi et al. (2008) reported that the pore-water velocity (*v*) of bromide was positively correlated with sand content. On the other hand, Vanderborght and Vereecken (2007) reported in their comprehensive literature evaluation that effect of texture on λ was not significant. They further stated that dispersivities were greater in saturated than unsaturated flow conditions in both fine- and coarse-textured soils.

The solute transport variables were also not significantly correlated with D_b, which we attributed to the fact that D_b may influence solute mobility differently in cropped, orchard, and grassland soils. Again, this does not match the findings of some previous studies. For example, Koestel et al. (2013) found a moderately significant positive correlation between D_b and both *v* and λ, which they attributed to increasing levels of D_b up to a certain value being related to increased near-saturated K_s, resulting in greater water saturation and the activation of larger macropores; while Mossadeghi-Björklund et al. (2016) reported that soil compaction had a significant detrimental effect on K_s and the number of macropores in one of their two study sites (but not at the other), and suggested that preferential flow would be strongest at an intermediate level of compaction.

These inconsistencies in the correlations between solute transport variables and soil properties between studies may be related to differences in the soil structure and effect of experimental conditions. Soil structure has previously been shown to affect the transport of water and dissolved chemicals (Beven and Germann, 1982; Chen and Wagenet, 1992), and critically influences solute transport in saturated soils (Jardine et al., 1988; Brusseau, 1993). Furthermore, preferential flow pathways have a strong control over solute transport in saturated and near-saturated soils, and are closely linked to soil structure (Kung et al., 2005). Supporting this, Ersahin et al. (2002) reported highly different *D* and *v* values for A, B_w, and E horizons of Tatuna Silt Loam (fine-silty, mixed, mesic, argiallbolls) in the Palouse region of Washington State due to soil structure differences. Because the parameter *D* is a property of the porous medium rather than the solute being transported (Nkedi-Kizza et al., 1983; Jardine et al., 1988; Brusseau, 1993), soil structure may offset the effects of soil properties such as soil texture, OM content, and bulk density on solute mobility in saturated and near-saturated conditions. For example, Lennartz et al. (1999) found a close relationship between bromide mobility and independently determined soil texture and OM content, but found almost no relationship between these when they considered non-preferential and preferential samples separately in a regression analysis, leading them to the conclusion that soil structure is an important property governing the preferential transport of solutes.

The cation exchange capacity was significantly correlated with log *v*, which may be attributed to the indirect effect of clays on this parameter. High positive correlations have previously reported between CEC and the specific surface area (SSA) (Ersahin et al., 2006; Bayat et al., 2015), and high SSA is generally related to the presence of 2:1-type clays that reduce saturated water flow (Sposito, 2008). There was also a significant weak correlation between the solute transport variables and $CaCO_3$ (Table 4). The $CaCO_3$ contents of the soils were between 0.1 and 12.65%, with a CV of 88%. $CaCO_3$ is known to be a good structure-forming agent in soil, increasing water flow in saturated and near-saturated conditions. That a negative significant correlation occurred between *R* and $CaCO_3$ may be attributed to indirect effect of $CaCO_3$ on *R* via soil pH since a moderate positive relation occurred between pH and $CaCO_3$ and a weak negative correlation occurred between pH and *R*.

Soil pH was also significantly correlated with log *v*. In our soils, the soil pH ranged from 5.73 to 8.55, with a mean of 7.59 (Table 3), and so this could be attributed to the detrimental effect of increased pH on anion adsorption, which results in increased bromide mobility. Furthermore, soil biological activity is also related to soil pH, which may also explain this significant correlation. There was some evidence of anion retardation in some of the columns as indicated by high *R*-values (the values for *R* ranged from 0.68 to 1.30), which may be attributed to the presence of variably charged particle surfaces. Soils containing kaolinite are expected to have positively charged surfaces at pH values below the point of zero charge (Sposito, 2008), which may result in anion

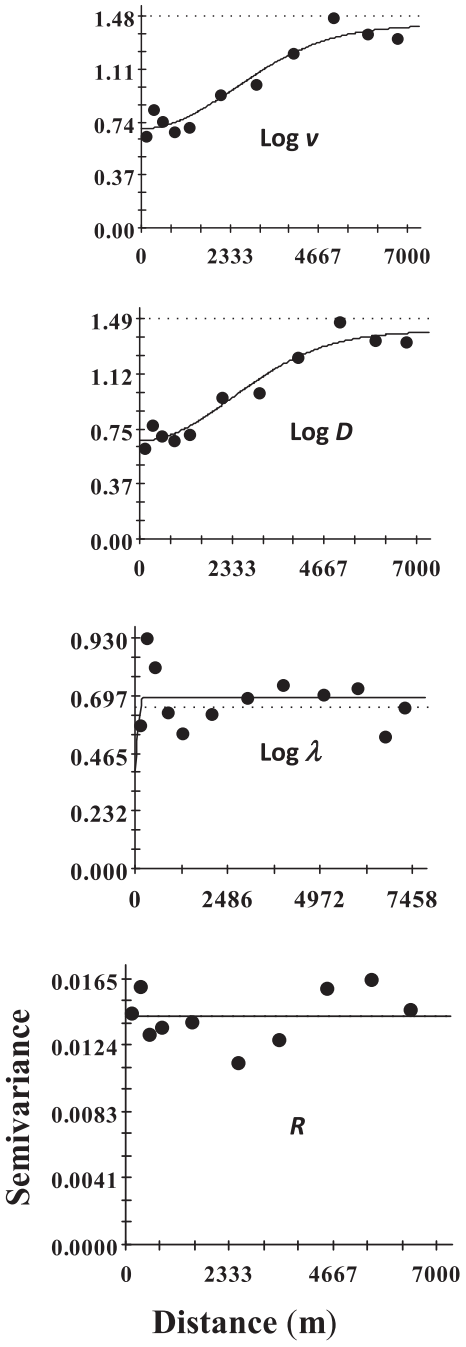

Fig. 3. Experimental (dots) and theoretical (line) semivariograms for log-transformed values of pore-water velocity (v), coefficient of hydrodynamic dispersion (D), dispersivity (λ), and untransformed values of retardation coefficient (R). The dashed lines show the general variance.

retardation. Bellini et al. (1996) showed that anion exchange capacity and Cl retardation decreased as pH increased in repacked columns of Pacolet series (clayey, kaolinitic, thermic Typic Kanhapludult); and Gillman and Sumner (1987) also reported anion exchange for Cecil soils due to a variable charge on kaolinite and oxides.

We found a significant relationship between land use and log λ. An ANOVA test ($P < 0.05$) showed that the mean of λ was greatest in grasslands, followed by orchards and cropped areas. We observed more biological activity (decayed root channels, earthworm channels, live earthworms, and voids) in grassland soils, and so attributed these differences for λ to higher levels of soil macropores and preferential flow

Table 5
Parameters of semivariograms for retardation coefficient (R) and log-transformed values of pore-water velocity (v), coefficient of hydrodynamic dispersion (D), and dispersivity (λ).

Variable	Model type	Nugget (C_0)	Sill (C)	C_0 / (C_0 + C)	Range (m)	R^2	RSS	r
Log_{10} v	Gaussian	0.67	1.40	0.47	5715.8	0.95	0.054	0.76
Log_{10} D	Spherical	0.27	1.38	0.20	520.0	0.94	0.062	0.87
Log_{10} λ	Spherical	0.57	0.69	0.83	222.0	0.077	0.14	0.02
R (−)	Linear	0.0131	0.0142	0.92	1812.8	0.14	4.14×10^{-5}	0.17

RSS: residual sum of squares, r: correlation coefficient for cross-validation, −: unitless.

paths, which could result in greater dispersivities in these soils. In addition, soil type was significantly correlated with R (Table 4), with ANOVA showing that the greatest mean value occurred in Typic Ustorthents followed by Mollic Ustifluvents and Lithic Ustipsamments (see Fig. 1 for their location in the study area). The ANOVA test further revealed that means of pH followed the reverse of that for R, indicating that pH was an important factor mediating the relationship between R and soil type.

Dispersivity (λ) is the ratio of dispersive transport to convective transport, with a greater value (e.g., >1) indicating a dispersive flow-dominated transport system and a smaller value (<1) indicating a convective flow-dominated transport system. In our study, the mean value for λ was 1.64 cm, with a standard deviation of 1.46 cm, a CV of 88%, a skewness of 2.92, and a kurtosis of 10.51, suggesting a highly kurtotic and right-skewed distribution (Table 2). Considerably different values of λ have been reported across laboratory column studies. Ersahin et al., (2002) reported λ mean values of 0.68, 1.03 and, 0.55 cm for undisturbed saturated columns of A, B_w, and E horizons of Thatuna silty loam (fine-silty, mixed, mesic Xeric Argiallbolls) under grassland, respectively. Bejat et al. (2000) reported values of 1.46 cm for intact tilled and 3.34 cm for intact sod blocks (32.5 by 32.5 by 32.5 cm) of Maurry silt loam; and 7.60 cm for tilled and 10.42 cm for sod intact blocks (32.5 by 32.5 by 32.5 cm) of Cecil sandy loam. Comegna et al. (2001) reported mean value of 2.83 cm for three intact soil samples (15 cm in diameter and 17 cm in length) collected from different sites in southern Italy. Gupte et al. (1996) reported a mean value of 6.6 cm and a CV of 41% for 38 intact columns (15 cm in internal diameter and 90 cm in length) of Cecil sandy loam (clayey, kaolinitic, thermic Typic Kanhapludult) and Vanderborght et al. (2000) reported λ-values ranging from 1.7 to 3.6 cm for intact sandy loam (Arenic Glossudalf) and from 3.9 to 16.1 cm for intact loam (Udifluvent on top of Hapludalf) columns.

Our mean value for λ was low compared to those reported by others (e.g., Vanderborght and Vereecken, 2007), and this may be attributed to several factors such as scale of the experiment, flow rate, and boundary conditions. In our study, all the leaching tests were conducted on saturated undisturbed columns. Vanderborght and Vereecken (2007) reported greater dispersivites, which they attributed to the effect of flow and transport through larger pores that are active in saturated soils. They further reported that dispersivity was scaled to vertical distance of travel, increased vertical distance resulting in increased values of λ. In our study, the column length was generally low (ranged from 12 to 30 cm with a mean of 19.7 cm and standard deviation of 6.01 cm) (see Fig. 2 for distribution of column length), which may explain the mainly low dispersivities we found.

Mean for v was 6.51 cm h^{-1} with a standard deviation of 10.33 cm h^{-1} (Table 2). The v-values were highly variable, strongly skewed to right and had a positively kurtotic distribution. Log-transformed values of v and λ were close to normal distribution, yet no significant correlation was found between them (Table 4). Despite to high v-values, the low dispersivities may be attributed to that we sampled the topsoil in cropped areas, orchards, and grasslands. Seventy-five of 100 samples were taken from cultivated areas (field cropped and orchards). The cultivated areas are tilled conventionally, which would induce

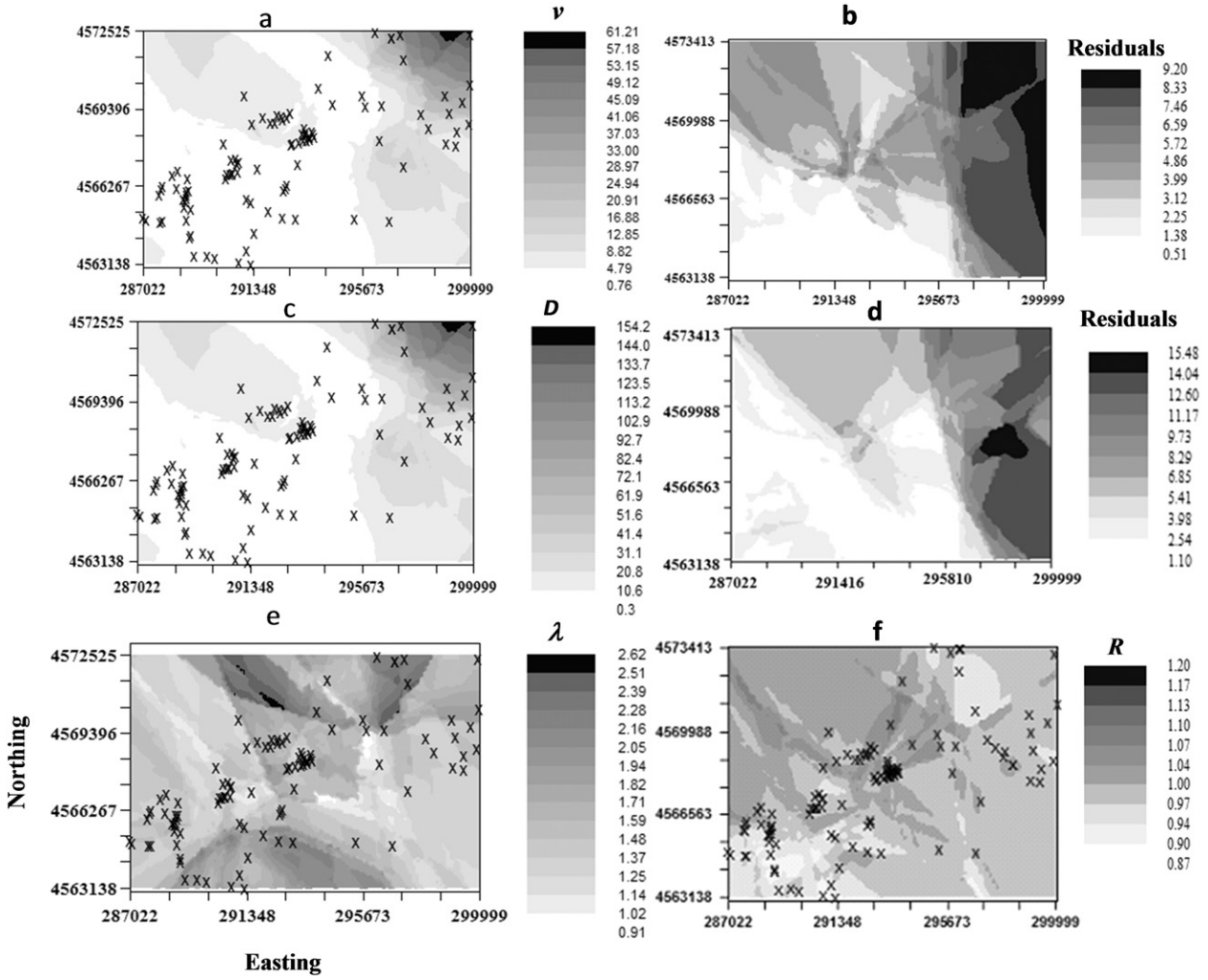

Fig. 4. Surface maps of a) ordinary kriging-interpolated pore-water velocity (v) values, b) 100 residuals calculated by cross-validation of v-values (interpolated-measured), c) ordinary kriging-interpolated values for coefficient of hydrodynamic dispersion (D), d) 100 residuals calculated by cross-validation of D-values (interpolated-measured), e) normal distance interpolated values of λ, and f) normal distance interpolated values of R. Absolute values of residuals were used in drawing the surface maps in b and d.

homogenization of the topsoil, resulting in low dispersivities as suggested by Vanderborght and Vereecken (2007).

A few soil columns exhibited high dispersivities (values for λ ranged from 0.05 to 9.15), indicating effect of preferential flow. Preferential flow is mainly generated by features such as macropores, root channels, and large inter-aggregate voids in soils (Jardine et al., 1988; Brusseau, 1993; Li and Ghodrati, 1994; Ersahin, 1996; Vanderborght and Vereecken, 2007). In majority of these columns, we observed earthworms and a strong subangular blocky structure at the time of sampling, as given in Table 1. The aggregate size and shape have a considerable effect on mass exchange between inter- and intra-aggregate spaces, particularly over the longer timeframes of miscible displacement (van Genuchten and Wierenga, 1977; Brusseau and Rao, 1990; Brusseau, 1993). For example, Li and Ghodrati (1994) reported a considerable macropore flow generated by decayed corn root channels.

The values for goodness of fit, R^2, ranged from 0.94 to 0.99 with a mean of 0.98 (Table 2), indicating that the convection-dispersion equation (CDE) described the breakthrough (BTC) data well. The BTC data from few columns with early breakthrough and late breakthrough were described by CDE with a R^2 below 0.95. However, majority of the BTC data were described by CDE with a R^2 >0.97.

Table 6
Descriptive statistics for interpolated values of pore-water velocity (v), coefficient of hydrodynamic dispersion (D), dispersivity (λ), retardation coefficient (R) in the study area ($n = 8715$).

Variable	Mean	Min	Max	SD	RMAE	r
v (cm h^{-1})[a]	7.98	0.76	61.21	9.80	0.087	0.76
D (cm^2 h^{-1})[a]	8.33	0.28	155.69	19.00	0.096	0.87
λ (cm)[b]	1.64	0.054	9.14	1.46	0.86	0.02
R (−)[b]	0.99	0.91	1.09	0.09	0.99	0.01

SD: standard deviation, RMAE: relative mean absolute error calculated using residuals of cross-validation: r: correlation coefficient of cross-validation, −: unitless.
[a] Interpolated by ordinary point kriging.
[b] Interpolated by normal distance weighted method.

5.2. Spatial variation in solute transport variables

We used semivariograms computed using log-transformed data of v, D, and λ and untransformed data of R to analyze their spatial structures. Variables v, D, λ, and R attained their maxima at geostatistical ranges of 5715, 520, 222 and 1812 m, respectively (Table 5, Fig. 3). Kazemi et al. (2008) previously reported geostatistical ranges of 20 and 23 m for v, and of 12 and 24 m for the D of bromide in a 0.1-ha alluvial field under no till management. By contrast, Gupte et al. (1996) reported that variograms of transport parameters showed no spatial dependence beyond the minimum spacing of 2.3 m on 12.5 × 30.5 m plots (clayey, kaolinitic, thermic, Typic Kanhapludult) based on 38 undisturbed soil samples collected from each. Koestel et al. (2013) also reported that the majority of BTC shape factors had a correlation distance below

15 m and that log-*v* had a correlation distance larger than 15 m in a topsoil (approximately 20 cm) of a 60 × 160-m agricultural field; and Ellsworth and Boast (1996) reported much smaller distances of autocorrelations for solute transport variables in a 2 × 2 × 2-m unsaturated field plot. Therefore, it is imperative that the sampling scheme, sampling resolution, and size of study area are considered when comparing geostatistical parameters to prevent the results from being misleading.

Our predictions for *v* and *D* based on randomly sampled soil cores from 100 sites had a satisfactory cross-validation statistical fit (Table 5), indicating that our sampling density was adequate to allow us to use geostatistical methods to map the spatial distribution of these parameters. However, this approach failed to correctly evaluate the spatial structures of *R* and λ, suggesting that denser sampling may be required to capture the complex signature of these parameters in the study area. Similar conclusions were previously made by Koestel et al. (2013).

Semivariogram models of the log data for *v* and *D* showed a moderate and strong spatial structure, respectively, as evidenced by their high nugget/sill ratio (Table 5) according to the criterion adopted by Cambardella et al. (1994). By contrast, Kazemi et al. (2008) reported moderate and strong spatial classes for bromide *v*, and a moderate spatial class for bromide *D*. The greatest structural variance occurred for *D*, for which the structural variance attributed 80% of the total variance with a range of 520 m (Table 5). By contrast, the structural variance attributed only 17% of the total variance for λ, and 8% for *R* at the current sampling scheme. The parameter λ is derived from *D*/*v*, and although both *v* and *D* were highly spatially dependent, λ had a very weak spatial dependency. This deserves a further studying.

There was no clear spatial structure for λ and *R* under the current sampling scheme. Spatial variation in solute transport attributes can be the product of the physical, chemical, and biological properties of the soil, as well as soil management practices such as tillage and cropping systems (Sauer and Meek, 2003). Dispersivity is strongly affected by the soil structure, texture, bulk density, soil macropores, plant roots, and other preferential pathways (van Genuchten and Wierenga, 1977; Nkedi-Kizza et al., 1983; Anamosa et al., 1990; Brusseau, 1993). In addition, λ is distance and time dependent at both the column and field scale (Wang et al., 2006; Vanderborght and Vereecken, 2007), which further complicates its spatial structure.

Typic Haplusteps and Mollic Ustifluvents occur on relatively gentle sideslopes (Fig. 1a), which are the product of spatially dependent weathering and erosional processes, as stated by Sauer and Meek (2003). However, regarding the different land uses, these soils differ in morphological properties such as soil structure, soil macropores, roots, etc. (Table 1). The physical and biological factors that dictate formation and destruction cycles of preferential pathways are highly variable both spatially and temporally (Kung et al., 2005). Therefore, these differences would result in considerable short-range spatial variation in solute dispersivity in these soils.

Surface maps for *v* and *D*, built using kriging (Fig. 4), show that the greatest values are located in the northeast (upper right part of their surface graphs) of the study area. These high valued localities are close to the seaside, where the soils are Lithic Ustipsamments, whereas the soils in the southwestern part of the study area, where *v* and *D* were generally low, are derived from co-alluvial parent material with a fine texture, and are mainly cultivated. In addition, soils in these areas are mainly rich in clay due to the fine-textured parent material. The cultivated lands in these areas are mainly used to grow field crops, such as sugar beets, corn, various vegetables, and alfalfa, and orchards of various fruits, such as cherries, hazelnuts, peaches, apples, and pears, with the northern part of the study area generally being under more diverse land uses than the southern part (see Fig. 1b). Therefore, the coarser soil texture and land use differences resulted in a greater variability in *v* and λ in the northern part of the study area.

The variables *v* and *D* were successfully interpolated by OK as indicated by adequately low relative mean absolute errors (RMAE) and high cross-validation correlation coefficients (Table 6). Ideally, a RMAE <0.1 indicates a good performance of subject model (Armstrong and Collopy, 1992). Spatial pattern for the kriging-cross validation residuals for *v* and *D* (Fig. 4) show that, in general, interpolation was more accurate in the southwest and around the center of the study area due to denser sampling and was less accurate in northeast of the study area due to sparser sampling. In addition, more diverse land use in the northern part of the study area would induce a greater short-range variation in *v* and *D*, resulting in the model to perform poorly in some localities. Both λ and *R* were interpolated by normal distance weighted method since their spatial structures were improper for their interpolation by kriging or inverse distance weighted at current sampling scheme and resolution.

6. Conclusions

In this study, we evaluated solute transport variables of, pore-water velocity (*v*), retardation coefficient (*R*), and dispersivity (λ = *D*/*v*) in adjacent Typic Haplusteps, Mollic Ustifluvents, and Lithic Ustipsamments and analyzed their spatial variation. In most of the study area, solute transport was dispersive dominated, with computed λ-values greater than unity. Some of the measured soil variables were significantly but weakly correlated with *v* and *D*, as were land use and soil type. In terms of land use, the greatest values of *v* occurred in grasslands, followed by orchards and cropped lands; while in terms of soil type, the greatest *v*-values occurred in Lithic Ustipsamments, followed by Mollic Ustifluvents, and Typic Ustorthents. Grassland soils tended to exhibit a well-aggregated strong structure, with the presence of continuous preferential flow pathways including macropores and soil morphological features such as continuous inter-aggregate spaces in these soils, which likely explains the higher values here. Our solute transport variables were not correlated with the physical properties of the soil, such as soil texture components, bulk density, and field capacity. However, soil chemical variables of cation exchange capacity, EC, pH, and $CaCO_3$ content were significantly correlated with the solute transport variables. Compared to those previously reported values, our values for λ were generally low, and this may be attributed to two principal reasons; 1) majority of the columns were short due to that the column length was limited by topsoil depth, resulting in a short vertical travel distance, which is scaled to λ (Vanderborght and Vereecken, 2007), and 2) 75 of 100 columns were taken from topsoil of cultivated areas, where the tillage could destroy preferential flow pathways and homogenize soils, resulting in smaller dispersivities as stated by Vanderborght and Vereecken (2007).

Pore-water velocity and coefficient of hydrodynamic dispersion (*D*) had distinct spatial structures using the applied sampling scheme, and ordinary kriging performed well in interpolating both *v* and *D*. However, λ and *R* exhibited a very different spatial pattern with far greater short-range variation, likely due to the greater number of factors that affect them. Therefore, denser sampling may be required to capture the more complex spatial signature of λ and *R* in the study area. This high short-range variation in *R* and λ should be considered in future studies that aim to analyze their spatial variation.

The findings of this study demonstrate that solute transport can be interpolated successfully over a large area with multiple land uses and soil types using geostatistical methods. This will be a tremendous advantage in land use planning that aims to reduce the risk of contamination of groundwater and surface water systems.

Acknowledgements

We thank The Scientific and Technological Research Council of Turkey (TUBITAK) for fully financing this study (Grant No: 108O348) and Director and staff of Black Sea Field Crop Research Institute for their help in soil sampling. We further thank two anonymous reviewers for their meticulousness and insightful comments.

References

Abdalla, N., Lear, B., 1975. Determination of inorganic bromide in soils and plant tissues with a bromide selective-ion electrode. Commun. Soil Sci. Plant Anal. 6, 489–494.

Anamosa, P.R., Nkedi-Kizza, P., Blue, W., Sartain, J., 1990. Water movement through an aggregated, gravelly oxisol from Cameroon. Geoderma 46, 263–281.

Armstrong, J.S., Collopy, F., 1992. Error measures for generalizing about forecasting methods: empirical comparison. Int. J. Forecast. 8, 69–80.

Bayat, H., Ebrahimi, E., Ersahin, S., Estela, N., Hepper, D.N.S., Amer, A.M., Yukselen-Aksoy, Y., 2015. Analyzing the effect of various soil properties on the estimation of soil specific surface area by different methods. Appl. Clay Sci. 116–117, 129–140.

Bejat, L., Perfect, E., Quisenberry, V.L., Coyne, M.S., Haszler, G.R., 2000. Solute transport as related to soil structure in unsaturated intact soil blocks. Soil Sci. Soc. Am. J. 64, 818–826.

Bellini, G., Sumner, M., Radcliffe, D., Qafoku, N., 1996. Anion transport through columns of highly weathered acid soil: adsorption and retardation. Soil Sci. Soc. Am. J. 60, 132–137.

Beven, K., Germann, P., 1982. Macropores and water flow in soils. Water Resour. Res. 18, 1311–1325.

Biggar, J., Nielsen, D., 1976. Spatial variability of the leaching characteristics of a field soil. Water Resour. Res. 12, 78–84.

Bowman, R., Rice, R., 1986. Transport of conservative tracers in the field under intermittent flood irrigation. Water Resour. Res. 22, 1531–1536.

Bresler, E., Laufer, A., 1974. Anion exclusion and coupling effects in nonsteady transport through unsaturated soils: II. Laboratory and Numerical Experiments. Soil Sci. Soc. Am. Proc. 38, 213–218.

Brusseau, M., 1993. The influence of solute size, pore-water velocity, and intraparticle porosity on solute dispersion and transport in soil. Water Resour. Res. 29, 1071–1080.

Brusseau, M., Rao, P., 1990. Modeling solute transport in structured soils: a review. Geoderma 46, 169–192.

Cambardella, C.A., Moorman, T.B., Novak, J.M., Parkin, T.B., Karlen, D.L., Turco, R.F., Konopka, A.E., 1994. Field-scale variability of central Iowa soils. Soil Sci. Soc. Am. J. 58, 1501–1511.

Cassel, D., Nielsen, D., 1986. Field capacity and available water capacity. In: Klute, A. (Ed.), Methods of Soil Analysis: Part 1—Physical and Mineralogical Methods. American Society of Agronomy and Soil Science Society of America, Madison, pp. 901–926.

Chen, C., Wagenet, R.J., 1992. Simulation of water and chemicals in macropore soils part 1. Representation of the equivalent macropore influence and its effect on soilwater flow. J. Hydrol. 130, 105–126.

Comegna, V., Coppola, A., Sommella, A., 2001. Effectiveness of equilibrium and physical non-equilibrium approaches for interpreting solute transport through undisturbed soil columns. J. Contam. Hydrol. 50, 121–138.

Corwin, D.L., Vaughan, P.J., 1997. Modeling nonpoint source of pollutants in vadose zone with GIS. Environ. Sci. Technol. 31, 2157–2176.

Costa, J.L., Prunty, L., 2006. Solute transport in fine sandy loam soil under different flow rates. Agric. Water Manag. 83, 111–118.

De Lucia, M., Legneau, V., de Fouquet, C., Bruna, R., 2011. The influence of spatial variability on 2D reactive transport simulations. Compt. Rendus Geosci. 343, 1–15.

Ellsworth, T.R., Boast, C.W., 1996. Spatial structure of solute transport variability in an unsaturated field soil. Soil Sci. Soc. Am. J. 60, 1355–1367.

Ersahin, S., 1996. Solute Transport in Sloping Layered Soils. Washington State University.

Ersahin, S., Papendick, R., Smith, J., Keller, C., Manoranjan, V., 2002. Macropore transport of bromide as influenced by soil structure differences. Geoderma 108, 207–223.

Ersahin, S., Gunal, H., Kutlu, T., Yetgin, B., Coban, S., 2006. Estimating specific surface area and cation exchange capacity in soils using fractal dimension of particle-size distribution. Geoderma 136, 188–197.

Fetter, C., 1993. Contaminant Hydrogeology. Macmillan Publishing Company, New York.

Flury, M., Flühler, H., Jury, W.A., Leuenberger, J., 1994. Susceptibility of soils to preferential flow of water: a field study. Water Resour. Res. 31, 2443–2452.

Gee, G., Bouder, J., 1986. Particle size analysis. In: Klute, A. (Ed.), Methods of Soil Analysis: Part 1. Physical and Mineralogical Methods. American Society of Agronomy and Soil Sicence Society of America, Madison, pp. 383–411.

Ghafoor, A., Koestel, J., Larsbo, M., Moeys, J., Jarvis, N., 2013. Soil properties and susceptibility to 18 preferential solute transport in tilled topsoil at the catchment scale. J. Hydrol. 492, 190–199.

Gillman, G., Sumner, M., 1987. Surface charge characterization and soil solution composition of four soils from the Southern Piedmont in Georgia. Soil Sci. Soc. Am. J. 51, 589–594.

Gregory, L.B., Grunwald, S., Osborne, T.Z., Reddy, K.R., Newman, S., 2006. Spatial distribution of soil properties in water conservation area 3 of the Everglades. Soil Sci. Soc. Am. J. 70, 1662–1676.

Gupte, S., Radcliffe, D., Franklin, D., West, L., Tollner, E., Hendrix, P., 1996. Anion transport in a piedmont ultisol: II. Local-scale parameters. Soil Sci. Soc. Am. J. 60, 762–770.

Isaaks, H., Srivastava, R., 1989. An Introduction to Applied Geostatistics. Oxford University Press, New York.

Iyigun, C., Türkeş, M., Batmaz, İ., Yozgatligil, C., Purutçuoğlu, V., Koç, E., Öztürk, M., 2013. Clustering current climate regions of Turkey by using a multivariate statistical method. Theor. Appl. Climatol. 114:95–106. http://dx.doi.org/10.1007/s00704-012-0823-7.

Jardine, P., Wilson, G., Luxmoore, R., 1988. Modeling the transport of inorganic ions through undisturbed soil columns from two contrasting watersheds. Soil Sci. Soc. Am. J. 52, 1252–1259.

Kazemi, H.V., Anderson, S.H., Goyne, K.W., Gantzer, C.J., 2008. Spatial variability of bromide and atrazine transport parameters for a udipsamment. Geoderma 144, 545–556.

Kelleners, T., Beekma, J., Chaudhry, M., 1999. Spatially variable soil hydraulic properties for simulation of field-scale solute transport in the unsaturated zone. Geoderma 92, 199–215.

Klute, A., Dirksen, C., 1986. Conductivity and diffusivity: laboratory methods. In: Klute, A. (Ed.), Methods of Soil Analysis: Part 1—Physical and Mineralogical Methods. American Society of Agronomy and Soil Science Society of America, pp. 687–734.

Koestel, J., Moeys, J., Jarvis, N., 2012. Meta-analysis of the effects of soil properties, site factors and experimental conditions on solute transport. Hydrol. Earth Syst. Sci. 16, 1647–1665.

Koestel, J.K., Norgaard, T., Luong, N.M., Vendelboe, A.L., Moldrup, P., Jarvis, N.J., Lamand, M., Iversen, B.V., Wollesen de Jonge, L., 2013. Links between soil properties and steady-state solute transport through cultivated topsoil at the field scale. Water Resour. Res. 49, 790–807.

Kung, K.-J.S., Hanke, M., Helling, C.S., Kladivko, E.J., Gish, T.J., Steenhuis, T.S., Jaynes, D.B., 2005. Quantifying pore-size spectrum of macropore-type preferential pathways. Soil Sci. Soc. Am. J. 69, 1196–1208.

Lennartz, B., Kamra, S.K., Meyer-Windel, S., 1999. Field scale variability of solute transport variability and related soil properties. Hydrol. Earth Syst. Sci. 4, 801–811.

Lessoff, S., Indelman, P., 2004. Analytical model of solute transport by unsteady unsaturated gravitational infiltration. J. Contam. Hydrol. 72, 85–107.

Li, Y., Ghodrati, M., 1994. Preferential transport of nitrate through soil columns containing root channels. Soil Sci. Soc. Am. J. 58, 653–659.

Matias, L.R., Bollero, G.A., Hoeft, R.G., Bullock, B.G., 2005. Spatial variability of the Illinois soil nitrogen test: implications for soil sampling. Soil Sci. Soc. Am. J. 97, 1585–1597.

McLean, E., 1982. Soil pH and lime requirement. In: Page, A., Miller, R., Keeney, D. (Eds.), Methods of Soil Analysis. Part 2. Chemical and Microbiological Properties. American Society of Agronomy and Soil Science Society of America, Madison, pp. 199–224.

Mossadeghi-Björklund, M., Arvidsson, J., Keller, T., Koestel, J., Lamandé, M., Larsbo, M., Jarvis, N., 2016. Effects of subsoil compaction on hydraulic properties and preferential flow in a Swedish clay soil. Soil Tillage Res. 156, 91–98.

Mulla, D., Mc Bratney, A., 2002. Soil spatial variability. In: Warrick, A. (Ed.), Soil Physics Companion. CRC Press, Boca Raton, pp. 343–373.

Mulla, D.J., McBratney, A.B., 2002. Soil spatial variability. In: Warrick, A.W. (Ed.), Soil Physics Companion, pp. 343–373 (Boca Raton).

Nelson, D., Sommers, L., 1982. Total Carbon, organic carbon, and organic matter. In: Page, A. (Ed.), Methods of Soil Analysis. Part 2. Chemical and Microbiological Properties. American Society of Agronomy and Soil Science Society of America, pp. 539–579.

Nkedi-Kizza, P., Biggar, J., van Genuchten, M., Th Wierenga, P., Selim, H., Davidson, J., Nielsen, D., 1983. Modeling tritium and chloride 36 transport through an aggregated oxisol. Water Resour. Res. 19, 691–700.

Parker, J., van Genuchten, M., 1984. Determining Transport Parameters from Laboratory or Field Tracer Experiments (Blacksburg).

Rhoades, J., 1982a. No title. In: Pages, A.L. (Ed.), Methods of Soil Analysis. Part 2. Chemical and Microbiological Properties. American Society of Agronomy and Soil Science Society of America, Madison, pp. 149–157.

Rhoades, J., 1982b. Soluble salts. In: Page, A. (Ed.), Methods of Soil Analysis. Part 2. Chemical and Microbiological Properties. American Society of Agronomy and Soil Science Society of America, Madison, pp. 167–179.

Sauer, T.J., Meek, D.W., 2003. Spatial variation of plant-available phosphorus in pastures with contrasting management. Soil Sci. Soc. Am. J. 67, 826–836.

Schoeneberger, P., Wysocki, D., Benham, E., Broderson, W. (Eds.), 2002. Field Book for Describing and Sampling Soils, second ed. Natural Resources Conservation Service, National Soil Survey Center, Lincoln.

Šimůnek, J., Van Genuchten, M.T., Šejna, M., Toride, N., Leij, F.J., 1999. The STANMOD Computer Software for Evaluating Solute Transport in Porous Media Using Analytical Solutions of Convection–Dispersion Equation.

Sposito, G., 2008. The Chemistry of Soils. Oxford University Press, New York.

Starr, J.L., Deroo, H.C., Frink, C.R., Parlange, J.-Y., 1978. Leaching characteristics of a layered field soil. Soil Sci. Soc. Am. J. 42, 386–391.

Toride, N., Leij, F., van Genuchten, M.T., 1995. The CXTFIT Code for Estimating Transport Parameters from Laboratory or Field Tracer Experiments (no. 137) (Riverside).

Trangmar, B., Yost, R., Uehara, G., 1985. Application of geostatistics to spatial studies of soil properties. Adv. Agron. (Riverside).

Van Eijkeren, J., Loch, J., 1984. Transport of cationic solutes in sorbing porous media. Water Resour. Res. 20, 714–718.

Van Genuchten, M.T., 1981. Non-equilibrium Transport Parameters From Miscible Displacement Experiments (Riverside).

van Genuchten, M., Wierenga, P., 1977. Mass transfer studies in sorbing porous media: I. Analytical solutions. Soil Sci. Soc. Am. J. 40, 473–480.

Vanclooster, M., Jawaux, M., Vanderborght, J., 2005. Solute transport in soil at the core and field scale. Encycl. Hydrol. Sci.

Vanderborght, J., Vereecken, H., 2007. Review of dispersivities for transport modeling in soils. Vadose Zone. J. 6:29–52. http://dx.doi.org/10.2136/vzj2006.0096.

Vanderborght, J., Timmerman, A., Feyen, J., 2000. Solute transport for steady-state and transient flow in soils with and without macropores. Soil Sci. Soc. Am. J. 64, 1305–1317.

Wang, H., Persaud, N., Zhou, X., 2006. Specifying scale-dependent dispersivity in numerical solutions of the convection–dispersion equation. Soil Sci. Soc. Am. J. 70, 1843–1850.

Ward, A., Gee, G., Zhang, Z., Keller, J., 2004. Vadose Zone Contaminant Fate-and-Transport Analysis for the 216-B-26 Trench.

Webster, R., 2001. Statistics to support soil research and their presentation. Eur. J. Soil Sci. 52, 331–340.

Zhang, Y., Gable, C.W., 2008. Two-scale modeling of solute transport in an experimental stratigraphy. J. Hydrol. 348, 395–411.